Algal Bloom Front Tracking Using an Unmanned Surface Vehicle: Numerical Experiments Based on Baltic Sea Data

Joana Fonseca*, Miguel Aguiar, João Borges de Sousa, and Karl H. Johansson

***Abstract*— We consider the problem of tracking moving algal bloom fronts using an unmanned surface vehicle (USV) equipped with a sensor that measures the concentration of chlorophyll *a*. Chlorophyll *a* is a green pigment found in plants, and its concentration is an indicator of phytoplankton abundance. Our algal bloom front tracking mission consists of three stages: deployment, data collection, and front tracking. At the deployment stage, a satellite collects an image of the sea from which the location of the front, the reference value for the concentration at this front and, consequently, the appropriate initial position for the USV are determined. At the data collection stage, the USV collects data points to estimate the local algal gradient as it crosses the front. Finally, at the front tracking stage, an adaptive algorithm based on recursive least squares fitting using recent past sensor measures is executed. We evaluate the performance of the algorithm and its sensitivity to measurement noise through MATLAB simulations. We also present an implementation of the algorithm on the DUNE onboard software platform for marine robots and validate it using simulations with satellite model forecasts from Baltic sea data.**

I. INTRODUCTION

Ocean ecosystems are greatly influenced by the structure and dynamics of fronts [1]. Detection and tracking of ocean fronts is important for investigating the formation, evolution, and interaction of ocean water masses [2], [3]. In this paper we develop an experimental setup capable of detecting and tracking ocean fronts using an unmanned surface vehicle (USV). Knowing the boundary between these water masses enables targeted sampling of the waters. An ocean front delineates the boundary between water masses distinguished by different physical, chemical, or biological characteristics. Some examples of ocean fronts are algae, salinity, and temperature fronts. A lack of efficient observations has hampered progress in understanding the dynamics of fronts. Global satellite measurements of ocean-surface velocities and air-sea fluxes, for instance, are only available at resolutions of a few hundred kilometers [4]. Therefore, the present paper suggests to approach data collection by using unmanned new sampling strategies for USVs. In fact, USVs can perform measurement runs over a long period of time at sea [5], which makes them a frequent choice for oceanographic data collection [6]. For this paper, the motivating scenario is harmful algal blooms (HABs), which occur frequently and cause significant damage. According to [7], "HABs cause human illness, large-scale mortality of fish, shellfish, mammals, and birds, and deteriorating water quality". To monitor and mitigate these detrimental effects, accurate information about the location and movement patterns of algal blooms are needed.

Front tracking has received an increasing amount of attention in the recent years. Ocean fronts are characterized by strong variations of some phenomena or variables such as algal blooms [8], salinity [9], temperature [10], Rhodamine dye [11], oil propagation [12], or other water properties. Front tracking can be divided into front estimation and vehicle control algorithms. Regarding front estimation, a variety of methods have been considered in the literature, such as model-based estimation for plume propagation [13] or local estimation of front direction [14]. Regarding vehicle control algorithms, we can find both multi-agent [15] and single-agent strategies [16], as well as adaptive algorithms for tracking depth [17] and non-adaptive zig-zag algorithms for tracking upwelling fronts [18], or velocity fronts [19]. While some tracking algorithms have been theoretically justified and proven to converge [20], [21], there is a lack of robustness guarantees in realistic setups, using local measurements of chlorophyll *a* concentration.

The main contribution of this paper is a numerical evaluation of an algal bloom front tracking strategy using Baltic sea data. An estimation algorithm for the gradient of chlorophyll *a* concentration, is proposed together with a control law for the USV heading. We define the front as a dynamic curve that corresponds to the level set of the chlorophyll *a* concentration with reference value obtained from satellite data. The USV records its position and the concentration at each position. The estimation is performed at each timestep in a receding-horizon fashion using the latest datapoints collected by the USV. The control input is a heading reference computed as a function of the estimated gradient, such that the USV moves towards the front when it is far away from it and along the front when it is close to it. The USV will remain within close proximity of the front after having reached it for the first time.

The paper is organised as follows. In Section II, the main problem is formulated and we give an overview of the components included in the experimental setup. We explain the front tracking algorithm in Section III. In Section IV, we describe the implementation of the algorithm, and sim-

*Corresponding author.

This work is supported by Knut and Alice Wallenberg Foundation, Swedish Research Council, and Swedish Foundation for Strategic Research.

J. Fonseca, M. Aguiar, and K. H. Johansson are with the Division of Decision and Control Systems, School of Electrical Engineering and Computer Science, and Digital Futures, KTH Royal Institute of Technology, SE-100 44 Stockholm, Sweden. {jfgf, aguiar, kallej}@kth.se.

J. Borges de Sousa is with the Underwater Systems and Technology Laboratory (LSTS), University of Porto, Portugal. jtasso@fe.up.pt.

ulations using satellite data of chlorophyll *a* concentration. Concluding remarks and future directions follow in Section V.

II. PROBLEM FORMULATION

We consider the problem of detecting and tracking irregular, moving, and time-varying algal bloom fronts. We propose a solution that consists of an experimental setup as in Fig. 1, composed of an USV with a chlorophyll *a* concentration sensor, a control and detecting algorithm implemented in the software platform DUNE [22], a message protocol implemented in IMC [23], a visualization tool implemented on Neptus [24], satellite data from the previous day, and the CMEMS simulated chlorophyll *a* data of the region from the past months [25].

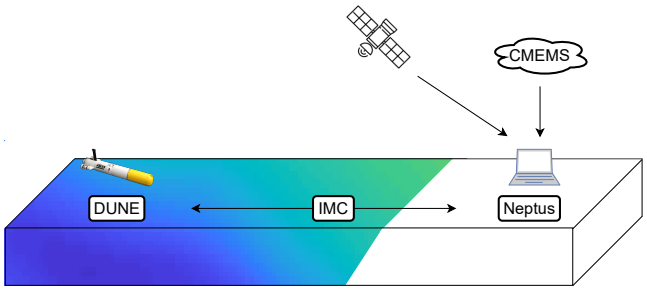

Fig. 1. Experimental setup including the USV, satellite, DUNE, IMC, and Neptus.

A. Algal blooms

In Fig. 2 we plotted two time instances of a forecasted chlorophyll *a* concentration field, part of the *Baltic Sea biogeochemistry analysis and forecast* product [25]. The spatial resolution is 2 km by 2 km, the time resolution is hourly, and we selected data from the east coast of Sweden, near Stockholm, from February 2020. The range from 0 (dark blue) to 1 (yellow) indicates the chlorophyll *a* concentration. The white areas represent land and correspond to the archipelago near Stockholm, Sweden.

We define a front (red) as a level set of a time-varying scalar field $\delta : \mathbb{R} \times \mathbb{R}^2 \to \mathbb{R}$:

$$F(t) = \{\mathbf{p} \in \mathbb{R}^2 : \delta(t, \mathbf{p}) = \delta_{\text{ref}}\}, \tag{1}$$

where δ_{ref} is some reference value, $\mathbf{p}$ the position and t time.

The reference δ_{ref} is chosen according to the latest satellite data of the location, before the mission starts. It can be seen as a calibration of the USV to different algal bloom situations.

B. Experimental setup

The components of the experimental setup are described next.

Satellite data – collected in the area of the experiment is used to initialize the controller, including the reference value and initial gradient estimate. CMEMS provides forecasts used for simulations before mission execution.

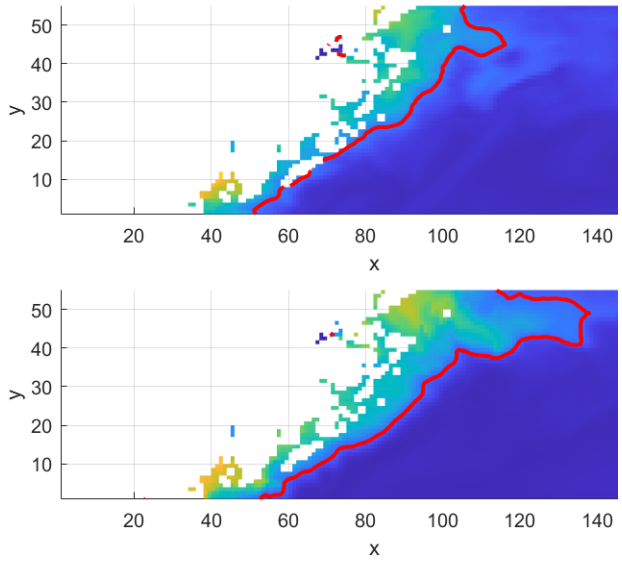

Fig. 2. CMEMS simulation data of chlorophyll *a* in the Baltic Sea, at two different time instances hours apart, with higher concentration (yellow), lower concentration (blue), land (white), and the front $F(t)$ (red line).

The **USV** – has a sensor to measure the concentration of chlorophyll *a*. See the UAV SAM from SMaRC (Swedish Maritime Robotics Centre, KTH [26]) with the Total Algae sensor from YSI [27] in Fig. 3.

Fig. 3. Top: SAM UAV from SMaRC. Bottom: Total Algae sensor from YSI

The **USV onboard software** contains the sensing, communications, navigation and control software used during the operation. For the implementation we used the LSTS toolchain that contains DUNE, IMC, and Neptus. For a detailed overview of the toolchain's components and capabilities, see [28]. DUNE is a platform- and architecture-independent runtime environment for the robot's onboard computer. It provides a simple and unified programming interface for writing embedded software components for marine robotics such as navigation filters, controllers or sensor drivers. Each software component is represented as a DUNE Task, an isolated code section which is executed in its own operating system thread. DUNE tasks communicate exclusively using IMC messages exchanged through a global shared message bus. Tasks can expose parameters (e.g, controller gains) which may be set in plain text configuration files and changed on-the-fly in the Neptus' operator console. DUNE contains an implementation of a navigation and control suite for the USV, as well as a detailed full-order USV

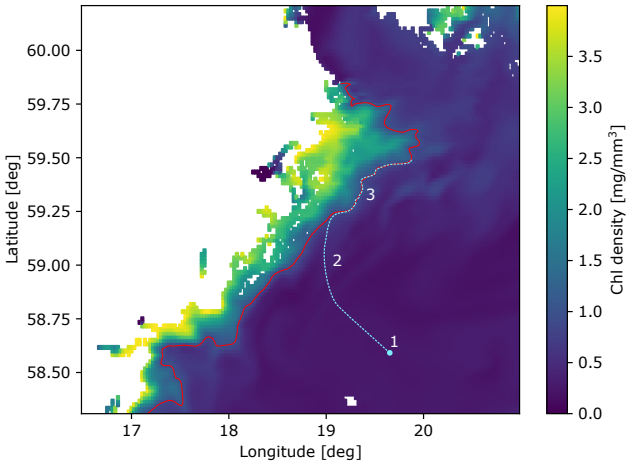

Fig. 4. Illustration of the three stages of the front tracking algorithm.

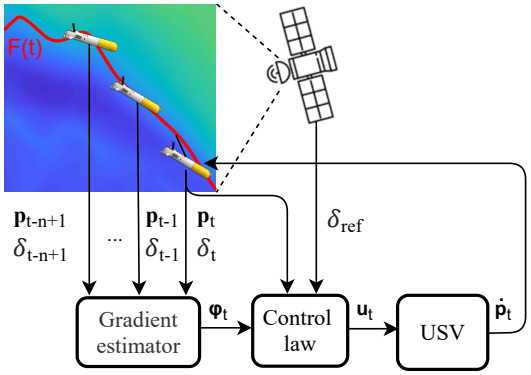

Fig. 5. USV control architecture

simulator. The simulator is used as a drop-in replacement of the sensor and actuator drivers which would interact with the real vehicle hardware, allowing us to simulate the same code that will later be deployed on the real robot.

The **mission control software** is used to monitor the system's position and operating state during the mission, and to retrieve collected data from the vehicle's storage. Neptus is a command and control application software providing a configurable and extensible graphical interface for mission planning and simulation, control, and review analysis.

Finally, the **mission control systems** are comprised of all the operators and support staff and systems involved in the mission. This may include research vessels or other types of manned or unmanned systems used to deploy and recover the USV.

C. Problem

The problem considered in this paper is how to track irregular and dynamic algal bloom fronts using the described experimental setup. The solution is a front tracking algorithm consisting of a control law, and a gradient estimator, as presented in the next Section.

III. FRONT TRACKING ALGORITHM

Given the problem stated above, we present a solution split into three stages, as illustrated in Fig 4. The first stage (indicated by 1 in the figure) is initialization and deployment aided by the satellite or forecast data, the second one (2) is finding and approaching the front, and the final one (3) is persistent front tracking.

The initialization stage consists in selecting the chlorophyll *a* reference value δ_{ref} and the vehicle's initial position and heading. We assume here that suitable values for these parameters can be obtained by examining satellite or forecast data corresponding to a point in time sufficiently close to the mission start time.

The front finding and approaching stage is lead by the control law which gives a velocity reference as a function of the measured chlorophyll *a* concentration at the vehicle's position. This velocity reference will lead the vehicle to the front location when it is away from the front and make the vehicle travel along the front when it is close to it. An essential ingredient in the control law is the gradient of the concentration, which is estimated from the measurements taken by the vehicle. The estimator computes an approximate value of the gradient at the vehicle's location using a local linear approximation of the chlorophyll *a* concentration. The final stage is the persistent front tracking which consists on keeping the USV in and around the front for the duration of the mission.

We summarize the overall architecture of the front tracking algorithm in Fig. 5. In the remaining subsections we give a detailed description of the control law, the gradient estimator, and the USV model.

A. Control Law

Assume for the moment that the reference value δ_{ref} is known and that the USV is holonomic, that is, the dynamics are given by

$$\dot{\mathbf{p}} = \mathbf{u},$$

where $\mathbf{p} = (x, y)$ is the vehicle's horizontal position and $\mathbf{u}$ is the velocity control. We define the feedback velocity law as:

$$\begin{aligned} \mathbf{u}(t,\mathbf{p}) &= \alpha_{\text{seek}}\mathbf{u}_{\text{seek}}(t,\mathbf{p}) + \alpha_{\text{follow}}\mathbf{u}_{\text{follow}}(t,\mathbf{p}) \\ \mathbf{u}_{\text{seek}}(t,\mathbf{p}) &= -(\delta(t,\mathbf{p}) - \delta_{\text{ref}})\nabla\delta(t,\mathbf{p}) \\ \mathbf{u}_{\text{follow}}(t,\mathbf{p}) &= R_{\pi/2}\nabla\delta(t,\mathbf{p}), \end{aligned} \tag{2}$$

where $\nabla\delta$ is the gradient of δ with respect to $\mathbf{p}$ and $R_{\pi/2}$ is a mapping which rotates vectors by 90 degrees. This feedback law has two components: the $\mathbf{u}_{\text{seek}}$ component controls the vehicle to the level set of δ corresponding to the front by following the gradient vector field, while $\mathbf{u}_{\text{follow}}$ makes the vehicle travel along the front. The direction in which the vehicle travels along the front after having reached it is determined by the orientation of $R_{\pi/2}$.

It can be seen that if the front F (in (1)) is static (i.e., $\partial\delta/\partial t \equiv 0$) then the feedback law $\mathbf{u}$ achieves convergence of the vehicle's position to the front (i.e. $\delta(t, \mathbf{p}(t)) \to \delta_{\text{ref}}$)

as long as $\nabla\delta \neq 0$, so that the vehicle does not get stuck in a critical point of δ. When the front is not static, there is no such guarantee. We assume that the vehicle is capable of moving and taking measurements at a time scale much faster than that at which the chlorophyll field is changing, so that we can view the time variation of δ as a perturbation.

B. Gradient estimator

In order to realize the control law (2), the gradient $\boldsymbol{\psi}(t) := \nabla\delta(t, \mathbf{p}(t))$ is needed. The vehicle takes noisy measurements of the concentration at discrete instants of time:

$$y_k = \delta(t_k, \mathbf{p}(t_k)) + \epsilon_k,$$

where t_k are the measurement times and ϵ_k is the measurement noise. We assume the position of the vehicle at the measurement times, $\mathbf{p}_k := \mathbf{p}(t_k)$ is perfectly known. We can then define the data available to the vehicle at time $t \in [t_k, t_{k+1})$ as

$$\mathcal{D}(t) = ((\mathbf{p}_0, y_0), (\mathbf{p}_1, y_1), \ldots, (\mathbf{p}_k, y_k)).$$

The gradient estimation problem is then to construct an estimate $\hat{\boldsymbol{\psi}}(t)$ of $\boldsymbol{\psi}(t)$ based on $\mathcal{D}(t)$.

We propose to construct such an estimate as follows. Let t_k be the time of the most recent measurement, and take n such that the set of measurements

$$\mathcal{D}_n(t) = ((\mathbf{p}_{k-n+1}, y_{k-n+1}), \ldots, (\mathbf{p}_k, y_k))$$

satisfies the following conditions:

- the measurements are taken suficiently close together in time so that the concentration is approximately constant on $[t_{k-n+1}, t_k]$;
- the measurements are taken close together in space.

These assumptions allow us to replace δ by its first order Taylor approximation on a set containing the measurement positions:

$$\delta(t, \mathbf{p}) \approx \delta(t^\star, \mathbf{p}^\star) + \nabla\delta(t^\star, \mathbf{p}^\star) \cdot (\mathbf{p} - \mathbf{p}^\star),$$

where $\mathbf{p}^\star$ is some position in this set and $t^\star \in [t_{k-n+1}, t_k]$ is some time instant. We define

$$\begin{aligned} \hat{\boldsymbol{\psi}} &= \nabla\delta(t^\star, \mathbf{p}^\star) \\ \delta_0 &= \delta(t^\star, \mathbf{p}^\star) - \nabla\delta(t^\star, \mathbf{p}^\star) \cdot \mathbf{p}^\star, \end{aligned}$$

so that

$$\delta(t, \mathbf{p}) \approx \delta_0 + \hat{\boldsymbol{\psi}} \cdot \mathbf{p}.$$

Applying this equation to the n measurements in $\mathcal{D}_n(t)$, we get a set of equations which are linear in δ_0 and $\hat{\boldsymbol{\psi}}$, which can be solved with standard least squares methods. An alternative is to use recursive least squares with exponential forgetting.

C. USV model

We adopt a typical 3 degree of freedom (surge, sway, and yaw) model for the USV [29]. It is represented as

$$\begin{aligned} \dot{\boldsymbol{\eta}} &= \mathbf{R}(\psi)\mathbf{v} \\ \boldsymbol{M}\dot{\mathbf{v}} + \boldsymbol{C}(\mathbf{v})\mathbf{v} + \boldsymbol{D}(\mathbf{v})\mathbf{v} &= \boldsymbol{\tau}, \end{aligned} \tag{3}$$

where $\boldsymbol{\eta} = [x, y, \psi]^T$ is the cartesian position $[x, y]$ and angle ψ, $\mathbf{v} = [u, v, r]^T$ are the velocities, and $\mathbf{R}(\psi) := \mathbf{R}_{z,\psi}$ is the rotational matrix.

IV. NUMERICAL EXPERIMENTS

A. MATLAB simulations

In this subsection we approximate the kinematics of the USV by a single integrator, $\dot{\mathbf{p}} = \mathbf{u}$. We simulated a 20 hour mission, having the length of saved data $\mathcal{D}_n(t)$ as $n = 20$ and the algal front concentration reference as $\delta_{\text{ref}} = 2$. Having measurements taken with a period of 3 minutes, we choose to start the gradient estimation after the first hour. We set the parameters $\alpha_{\text{seek}} = 6$ and $\alpha_{\text{follow}} = 2$ of the control law $\mathbf{u}(t)$. We deploy the USV at $\mathbf{p}(0) = [65, 1]$ with an initial algal gradient estimate of $\hat{\boldsymbol{\psi}}(0) = [1, -1]$. We introduce a measurement error in the chlorophyll *a* sensor of the form $\delta_{\text{measured}}(t) = \delta_{\text{real}}(t) + \delta_{\text{noise}}(t)$ with maximum noise of about 0.4.

Fig. 6 shows six instances of the algal front tracking mission. From the first one, we can see the initial position at which the USV was deployed, as well as its convergence towards the algal front $F(t)$. The following figures indicate a constant and accurate tracking of the algal bloom front. Here, we can also see the gradient estimator $\hat{\boldsymbol{\psi}}$ indicating a fair estimation of the normal vector to the algal front on the USV's position.

Tracking and estimation errors are depicted in Fig. 7. The first figure contains three chlorophyll *a* concentration values: the measurement $\delta_{\text{measured}}(t)$, the real chlorophyll *a* concentration $\delta(t)$, and the reference δ_{ref}. The oscillation around the reference value represents the deviation to the front. Here we can notice two things: first, the measured and real values have a difference corresponding to the sensor noise; second, the USV starting point is far from the front, but it then oscillates around the reference value of chlorophyll *a* concentration.

The second figure illustrates the distance of the USV to the closest point of the front $F(t)$: $\inf_{f \in F(t)} \|f - \mathbf{p}(t)\|$. Here, the initial distance is large as the USV is starting far from the front. Then, the distance oscillates around zero, indicating a zig-zag motion around the front. The last figure depicts the angle of the estimated gradient, $\angle\boldsymbol{\psi}(t)$. By plotting the angle, we can evaluate the variation of directions towards the front $F(t)$.

B. DUNE controller implementation

In the DUNE control implementation, a two-step waypoint generation scheme is used, where the robot performs a 'zig-zag' motion of amplitude θ and horizontal displacement d

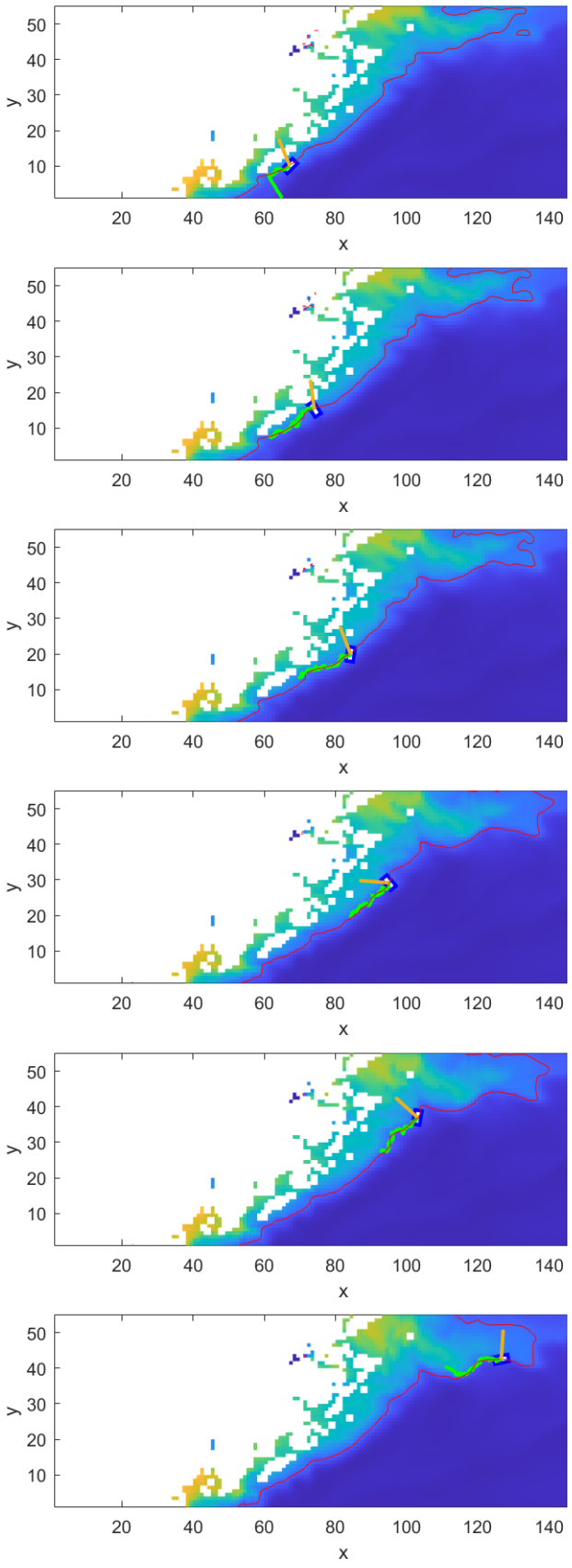

Fig. 6. Time-lapse of the USV (blue rectangle) and its gradient estimator $\boldsymbol{\psi}$ (red arrow) tracking the algal front (indicated with red contour lines)) with representation of USV's path (green).

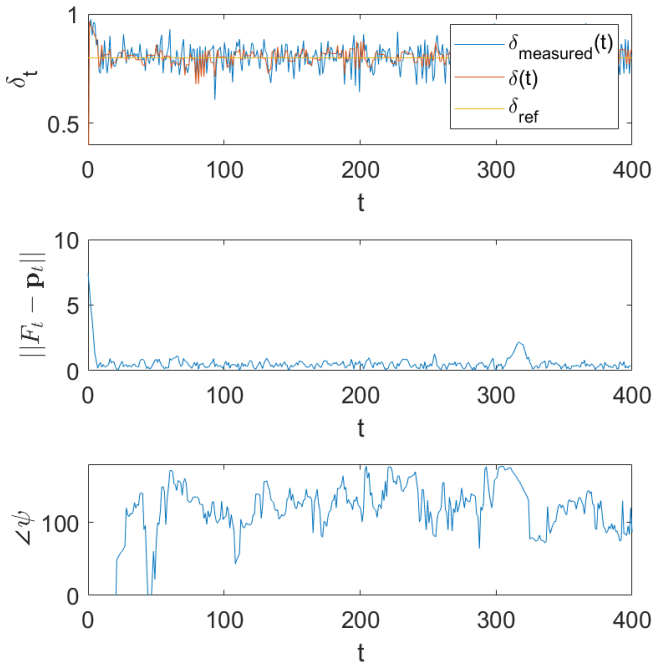

Fig. 7. First plot: difference between the noisy measured chlorophyll a concentration $\delta_{\text{measured}}(t)$, local chlorophyll a concentration $\delta(t)$, and the reference chlorophyll a concentration δ_{ref}. Second plot: distance from the USV to the closest point in the front, $\|F(t) - \mathbf{p}(t)\|$. Third plot: angle of the estimated gradient, $\angle\boldsymbol{\psi}(t)$.

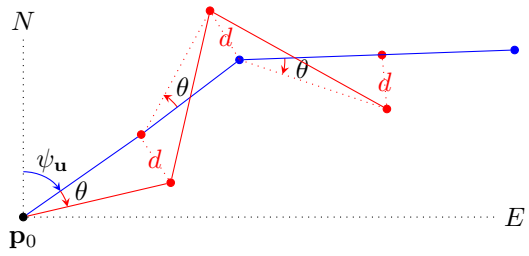

Fig. 8. Waypoint generation scheme.

around a mean bearing angle $\psi_{\mathbf{u}}$. This is depicted in Fig. 8. After the vehicle reaches the second waypoint, the measurements collected during the motion are used to estimate the gradient as described above, and a new bearing reference $\psi_{\mathbf{u}}$ is computed using (2). The vehicle travels at constant speed, so that only the relative size of α_{seek} and α_{follow} in (2) is relevant, and we fix $\alpha_{\text{follow}} = 1$. The value of δ used in the computation of $\mathbf{u}$ is the most recent sample.

As above, the gradient estimate $\hat{\boldsymbol{\psi}}$ is initialized with a given value. Gradient estimation is performed only after the average concentration is within a threshold error δ_{thr} of δ_{ref},. Thus, initially the vehicle travels in a straight line (i.e., $d, \theta = 0$) and a fixed track distance is used to compute the next waypoint, with the track bearing given by (2).

The chlorophyll a concentration field is simulated using numerical data defined on a regular time-latitude-longitude grid. A DUNE task simulating the chlorophyll a concentra-

tion sensor reads messages containing the vehicle's current position, linearly interpolates the numerical data to the vehicle position and current time and dispatches an IMC message containing the current concentration value. These messages are then read by the controller task which stores them together with the corresponding vehicle position.

C. DUNE simulation results

α_{follow}	d	θ	Speed	δ_{ref}	δ_{thr}
25	250 m	45 deg.	5 m/s	1 mg/m^3	0.1 mg/m^3

TABLE I

CONTROLLER PARAMETERS USED IN THE DUNE SIMULATION.

We simulated an approximately 32 hour mission with the controller parameters shown in Table I. The vehicle samples the chlorophyll *a* concentration at its position every 3 seconds with Gaussian measurement noise of variance 0.001 mg/m^3. Fig. 9 shows the position of the vehicle and the chlorophyll *a* concentration field at two instants of time. Blue regions indicate low concentration values at the corresponding position, while green regions indicate high concentration values. The red curves represent the front $F(t)$ at the corresponding time instant. After the initial approach phase the vehicle successfully tracks the time-varying front.

Fig. 10 shows the chlorophyll *a* concentration measured by the vehicle, normalized to the maximum value contained in the data. The shaded blue area indicates the value of δ_{thr}. One can see that the vehicle loses track the front at around $t = 18$ h. This is because the chlorophyll field changes significantly between $t = 18$ h and $t = 19$ h, so that the assumptions considered in the estimator design are no longer valid. After this sudden change the vehicle recovers the front and tracks it successfully again, showing that the algorithm is robust to temporary violations in the assumptions.

V. CONCLUSIONS

In this paper we considered the problem of algal bloom front tracking using a sensing USV. We assumed the USV has a GPS receiver which reports its position, and a chlorophyll *a* concentration sensor which measures the local algal concentration. We proposed an experimental setup composed of satellite data, USV hardware and software, CMEMS forecasted data, and an algorithm in which the USV estimates the local algal gradient using recent past measurements and least squares fitting. We provided a MATLAB simulation and analyzed convergence given sensor noise. The USV converged and moved along the detected algal bloom front for the duration of the mission. The algorithm was also implemented on the LSTS Toolchain using model forecasts of the chlorophyll *a* concentration in the Baltic Sea in February 2020 from CMEMS.

Our future plan is to do tests on the Baltic Sea using our algorithm implemented on DUNE and Neptus as well as algal bloom forecasting using satellite data of different water properties, such as salinity, temperature, and water currents.

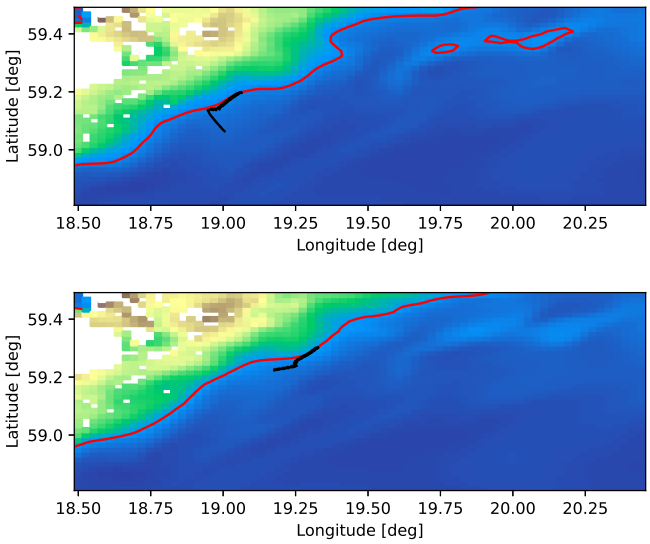

Fig. 9. Two time instants ($t = 10$ h and 25 h) of the mission. The black line shows the USV path over the preceding 10 hours.

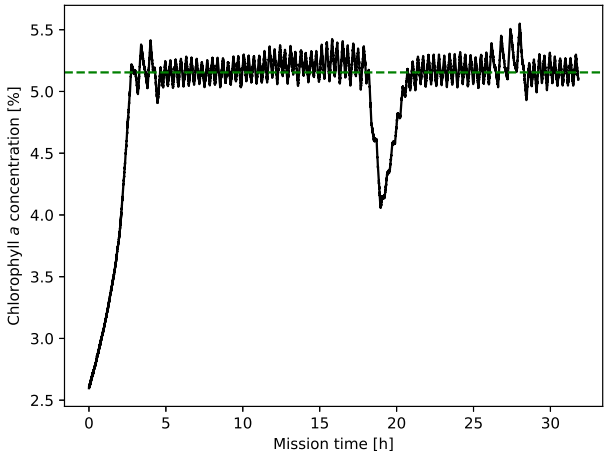

Fig. 10. Chlorophyll *a* concentration measured by the vehicle.

We would like to thank CMEMS for providing the data used in the experimental evaluations in this paper.

REFERENCES

[1] J. P. Ryan, A. M. Fischer, R. M. Kudela, M. A. McManus, J. S. Myers, J. D. Paduan, C. M. Ruhsam, C. B. Woodson, and Y. Zhang, "Recurrent frontal slicks of a coastal ocean upwelling shadow," *Journal of Geophysical Research: Oceans*, vol. 115, no. C12, 2010.

[2] R. N. Smith, Y. Chao, P. P. Li, D. A. Caron, B. H. Jones, and G. S. Sukhatme, "Planning and implementing trajectories for autonomous underwater vehicles to track evolving ocean processes based on predictions from a regional ocean model," *The International Journal of Robotics Research*, vol. 29, no. 12, pp. 1475–1497, 2010.

[3] R. N. Smith, M. Schwager, S. L. Smith, B. H. Jones, D. Rus, and G. S. Sukhatme, "Persistent ocean monitoring with underwater gliders: Adapting sampling resolution," *Journal of Field Robotics*, vol. 28, no. 5, pp. 714–741, 2011.

[4] R. Ferrari, "A frontal challenge for climate models," *Science*, vol. 332, no. 6027, pp. 316–317, 2011.

[5] R. Millet, F. Plumet, and J.-C. Dern, "Autonomous surface vehicle for oceanographic survey," 2008.

[6] Z. Liu, Y. Zhang, X. Yu, and C. Yuan, "Unmanned surface vehicles: An overview of developments and challenges," *Annual Reviews in Control*, vol. 41, pp. 71 – 93, 2016.

[7] S. Shumway, J. M Burkholder, and S. Morton, *Harmful Algal Blooms: A Compendium Desk Reference*, 2018.

[8] Y.-H. Ahn, P. Shanmugam, J.-H. Ryu, and J.-C. Jeong, "Satellite detection of harmful algal bloom occurrences in korean waters," *Harmful Algae*, vol. 5, no. 2, pp. 213–231, 2006.

[9] I. Belkin, J. Sousa, J. Pinto, R. Mendes, and F. López-Castejón, "A new front-tracking algorithm for marine robots," *2018 IEEE/OES Autonomous Underwater Vehicle Workshop (AUV)*, pp. 1–3, 2018.

[10] Y. Zhang, C. Rueda, B. Kieft, J. P. Ryan, C. Wahl, T. C. O'Reilly, T. Maughan, and F. P. Chavez, "Autonomous tracking of an oceanic thermal front by a wave glider," *Journal of Field Robotics*, vol. 36, no. 5, pp. 940–954, 2019.

[11] Wei Li, J. A. Farrell, Shuo Pang, and R. M. Arrieta, "Moth-inspired chemical plume tracing on an autonomous underwater vehicle," *IEEE Transactions on Robotics*, vol. 22, no. 2, pp. 292–307, 2006.

[12] M. Fahad, N. Saul, Y. Guo, and B. Bingham, "Robotic simulation of dynamic plume tracking by unmanned surface vessels," in *2015 IEEE International Conference on Robotics and Automation (ICRA)*, 2015, pp. 2654–2659.

[13] S. Li, Y. Guo, and B. Bingham, "Multi-robot cooperative control for monitoring and tracking dynamic plumes," in *2014 IEEE International Conference on Robotics and Automation (ICRA)*, 2014, pp. 67–73.

[14] Y. Zhang, B. Kieft, B. W. Hobson, J. P. Ryan, B. Barone, C. M. Preston, B. Roman, B. Y. Raanan, R. Marin III, T. C. O'Reilly, C. A. Rueda, D. Pargett, K. M. Yamahara, S. Poulos, A. Romano, G. Foreman, H. Ramm, S. T. Wilson, E. F. DeLong, D. M. Karl, J. M. Birch, J. G. Bellingham, and C. A. Scholin, "Autonomous tracking and sampling of the deep chlorophyll maximum layer in an open-ocean eddy by a long-range autonomous underwater vehicle," *IEEE Journal of Oceanic Engineering*, vol. 45, no. 4, pp. 1308–1321, 2020.

[15] A. Branch, M. M. Flexas, B. Claus, A. F. Thompson, Y. Zhang, E. B. Clark, S. Chien, D. M. Fratantoni, J. C. Kinsey, B. Hobson, B. Kieft, and F. P. Chavez, "Front delineation and tracking with multiple underwater vehicles," *Journal of Field Robotics*, vol. 36, no. 3, pp. 568–586, 2019.

[16] Y. Zhang, M. Godin, J. Bellingham, and J. Ryan, "Using an autonomous underwater vehicle to track a coastal upwelling front," *IEEE Journal of Oceanic Engineering*, vol. 37, pp. 338–347, 2012.

[17] R. N. Smith, P. Cooksey, F. Py, G. S. Sukhatme, and K. Rajan, *Adaptive Path Planning for Tracking Ocean Fronts with an Autonomous Underwater Vehicle*. Cham: Springer International Publishing, 2016, pp. 761–775.

[18] Y. Zhang, J. G. Bellingham, J. P. Ryan, B. Kieft, and M. J. Stanway, "Autonomous four-dimensional mapping and tracking of a coastal upwelling front by an autonomous underwater vehicle," *Journal of Field Robotics*, vol. 33, no. 1, pp. 67–81, 2016.

[19] D. Kularatne, R. N. Smith, and M. A. Hsieh, "Zig-zag wanderer: Towards adaptive tracking of time-varying coherent structures in the ocean," in *2015 IEEE International Conference on Robotics and Automation (ICRA)*, 2015, pp. 3253–3258.

[20] J. Fonseca, J. Wei, K. H. Johansson, and T. A. Johansen, "Cooperative decentralized circumnavigation with application to algal bloom tracking," in *in IEEE International Conference on Intelligent Robots and Systems (IROS)*, 2019, p. 3276–3281.

[21] J. Fonseca, J. Wei, T. A. Johansen, and K. H. Johansson, "Cooperative circumnavigation for a mobile target using adaptive estimation," in *CONTROLO 2020*. Cham: Springer International Publishing, 2021, pp. 33–48.

[22] [Online]. Available: https://lsts.fe.up.pt/software/64

[23] [Online]. Available: https://www.lsts.pt/docs/imc/master/

[24] [Online]. Available: https://lsts.fe.up.pt/software/54

[25] [Online]. Available: https://marine.copernicus.eu/about-us/about-eu-copernicus/

[26] [Online]. Available: https://smarc.se

[27] [Online]. Available: https://www.ysi.com/pro/talpc

[28] J. Pinto, P. S. Dias, R. Martins, J. Fortuna, E. Marques, and J. Sousa, "The LSTS toolchain for networked vehicle systems," in *2013 MTS/IEEE OCEANS - Bergen*, 2013, pp. 1–9.

[29] T. I. Fossen, *Handbook of Marine Craft Hydrodynamics and Motion Control*. John Wiley & Sons, Ltd, 2011.